Motion Simulation

Dealing with the Ill-Conditioned Equations of Motion for Articulated Figures

Anthony A. Maciejewski
Purdue University

Realistic motion simulation for articulated figures has generated a great deal of interest in recent years. Whether the simulation is based on the kinematics or the dynamics of the figure, most formulations rely on the solution of linear systems of equations. Sometimes solution of these equations presents a great deal of numerical difficulty, resulting in unrealistic or spurious motion for the figure or in excessive computation because of small integration intervals.

This article shows the cause of the difficulty to be related to the physical structure of the figure, not the mathematical formulation. It also shows how to determine the severity of ill conditioning and how to obtain physically meaningful solutions without excessive computations, even when dealing with extremely ill-conditioned configurations.

The importance of the computer graphic simulation of articulated figures has been demonstrated by *CG&A*'s two special issues on the topic[1-6] and SIGGRAPH's regular courses and technical sessions on this or related areas.[7-14] Much literature has been devoted to this topic in other disciplines—perhaps most notably robotics, where there are similarities in the problem formulation. Throughout much of this work, the issue of numerical stability and conditioning arises, primarily because providing an efficient and robust implementation of a digital simulation is difficult.[5-10,13-18] Such problems are for the most part universal, regardless of whether the figures are biological or mechanical, or whether the simulation is kinematic or dynamic. This article identifies the source of the ill conditioning in the equations of motion for articulated figures and provides robust numerical techniques for alleviating the difficulties that they create.

It is important first to distinguish between numerical instability and ill conditioning. Numerical instability refers to the errors introduced into computations by the numerical techniques used. In contrast, ill conditioning refers to the unavoidable uncertainty arising from the nature of the problem being solved. The ill conditioning that arises in the

0272-17-16/90/0500-0063$01.00 ©1990 IEEE

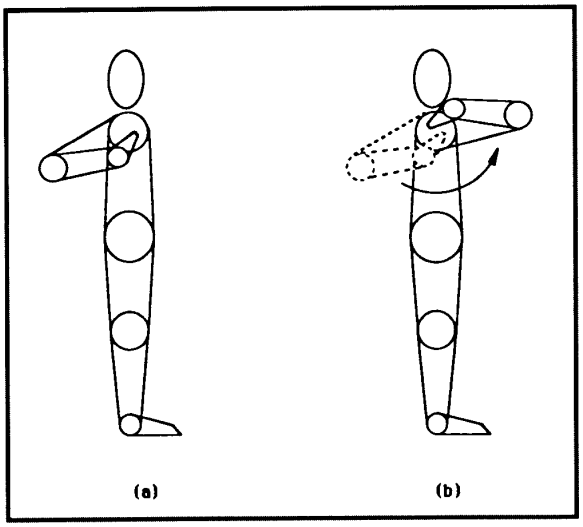

Figure 1. The equations of motion relating the position of the hand to the positions of the shoulder, elbow, and wrist joints, perpendicular to the sagittal plane, are ill conditioned. A small change in the position of the hand from (a) to (b) requires a large change in the position of the shoulder joint.

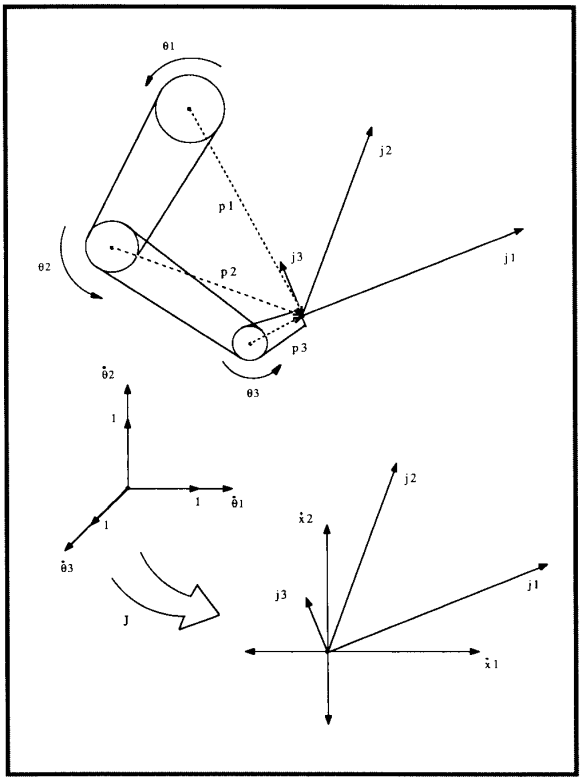

Figure 2. A physical interpretation of the columns of the Jacobian matrix that describes the kinematic transformation between the joint velocities and the velocity of the hand.

equations of motion for most articulated figures is inherent in the figures' physical structure and not due to a choice in mathematical formulation.

As a simple example, consider the motion of the human arm in the sagittal plane illustrated in Figure 1. If the hand is to be placed slightly under the shoulder as in Figure 1a, the elbow must be located behind the back of the figure. If the hand is slightly over the shoulder as in Figure 1b, the elbow must be in front of the figure. Thus, for an extremely small change in the position of the hand, the joint in the shoulder must traverse through its entire range of motion. Determining the required position of the shoulder joint when given the position of the hand is not a well-posed problem; that is, it is ill conditioned. If there is any small variation in the calculation of the hand's position, as is inevitable with digital arithmetic, the error is magnified. The resulting shoulder motion will exhibit oscillations and physically unrealistic accelerations.

This example illustrates the inherent ill conditioning in the kinematic transformation between hand coordinates and joint coordinates. An analogous difficulty arises in the dynamic equations of motion relating the torques at the joints to their accelerations. This article considers in detail how to analyze sources of ill conditioning, how to determine the severity of the problem, and what numerical techniques to apply to ill-conditioned formulations. The presentation relies primarily on kinematic examples for two reasons: They tend to be easier to visualize, and they must deal with the added difficulty of singularities. The equations of motion for a dynamic simulation cannot be singular unless physically unrealistic bodies of zero or negative mass are allowed. The article concludes with an example of how the techniques discussed can be applied to dynamics simulations, and how they relate to previous methods.

Problem formulation

A fundamental problem in motion simulation for articulated figures is how to determine the values for the parameters that can be controlled, so a desired motion results. In kinematic simulations the desired motion is typically defined as a trajectory for some part of a limb (e.g., a hand), and the controllable variables are the joints in the limb. The relationship between these trajectories can be specified as positions, velocities, accelerations, or even higher order deriva-

tives. Using velocities is particularly convenient, because we can avoid the typically nonlinear relationship between positions.

Consider once again the motion of the human arm in the sagittal plane, where desired trajectories are given for the hand (see Figure 2). The relationship between the velocity of the hand, denoted by the 2D vector $\dot{\mathbf{x}}$, and the joint velocities, denoted by the 3D vector $\dot{\theta}$, is given by

$$\dot{\mathbf{x}} = \mathbf{J}\dot{\theta} \tag{1}$$

where $\mathbf{J}$ is known as the Jacobian matrix and is conveniently represented by its columns as

$$\mathbf{J} = [\, \mathbf{j}_1 \, \mathbf{j}_2 \, \mathbf{j}_3 \,] \tag{2}$$

The columns of $\mathbf{J}$ have a simple physical interpretation, because they are the resulting hand velocities for a unit rotational velocity at each of the respective joints. They can be easily calculated by noting that they are closely related to the vector defined from a joint's axis to the hand, denoted by $\mathbf{p}_i$ ($\mathbf{p}_1$, $\mathbf{p}_2$, and $\mathbf{p}_3$ in Figure 2). In particular, the magnitudes of the $\mathbf{j}_i$'s and $\mathbf{p}_i$'s are equal, and their directions are perpendicular. This relation is easily extended to three dimensions using the cross product of a unit vector along the axis of rotation with the vector $\mathbf{p}_i$ to obtain $\mathbf{j}_i$.[17]

The above description shows that the velocity produced at the hand by a given joint velocity will vary, depending on the configuration of the arm. This fact is sometimes emphasized by explicitly denoting the Jacobian's dependence on the joint angles by writing $\mathbf{J}(\theta)$. For most configurations some hand velocities are easier to achieve than others; that is, they require lower joint velocities. This information is closely related to the conditioning of $\mathbf{J}$ and to the amount of error that can be expected when solving Equation 1. Singular value analysis provides a powerful tool for determining strict bounds on this error and for characterizing the Jacobian transformation.

Singular value analysis

Considering the Jacobian as composed of columns provides an intuitive interpretation for how the hand moves when individual joints are moved. The joints of articulated figures, however, are very seldom moved one at a time. Most frequently some combination of all joints must be moved to achieve a desired trajectory. To characterize the Jacobian transformation under these conditions, consider the set of all possible different combinations of joint velocities of unit magnitude. This can be represented as a sphere in joint space, as illustrated in Figure 3. Because of the directionally dependent scaling of the Jacobian transformation, the velocity at the hand resulting from all these possible inputs will generally be described by an ellipse. This ellipse graphically depicts the directions in which the hand can move more easily.

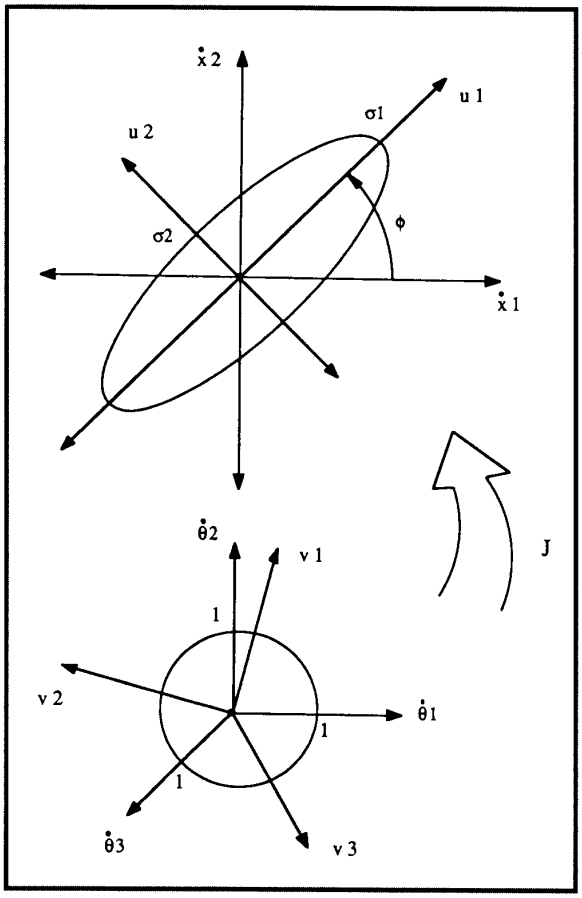

Figure 3. A geometric interpretation of the singular value decomposition as applied to the Jacobian transformation illustrated in Figure 2.

Note at this point that the choice of coordinate systems for the hand is rather arbitrary and can be changed to any convenient set. Since the axes of the ellipse describing the hand velocities for all possible joint inputs have a physical significance, they represent an ideal choice. These new axes will be denoted $\hat{\mathbf{u}}_1$ and $\hat{\mathbf{u}}_2$ for the major axis and minor axis, respectively. This new coordinate system can be viewed as a simple rotation of the old coordinate system by an

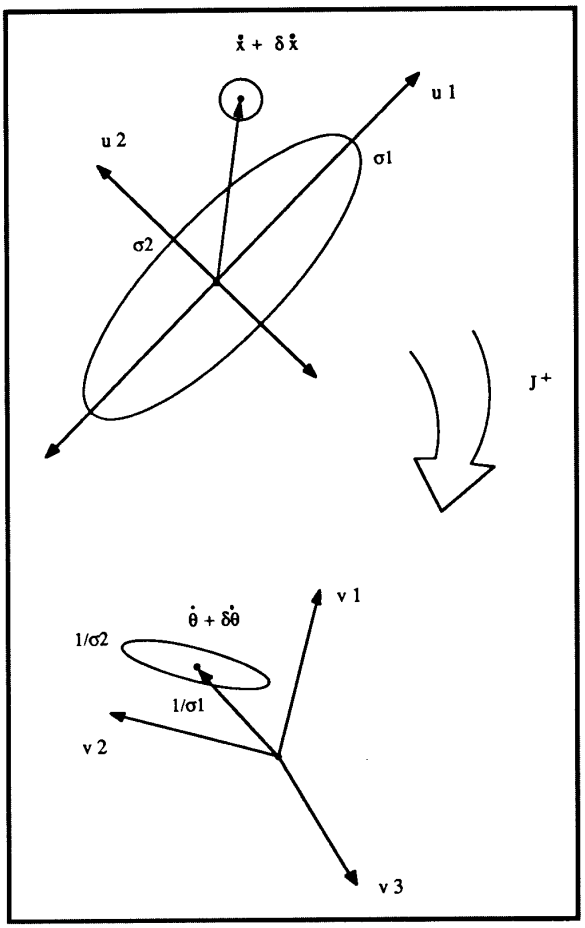

Figure 4. The transmission of relative uncertainty in the velocity of the hand to uncertainty in the calculated velocity of the joints. The range of this uncertainty is given by the ratio of the largest to the smallest singular values and is the definition of the condition number.

angle ϕ, so vectors defined in one system can be transformed to the other using the rotation matrix **U** given by

$$\mathbf{U} = [\,\hat{\mathbf{u}}_1\ \hat{\mathbf{u}}_2\,] = \begin{bmatrix} \cos\varphi & \sin\varphi \\ -\sin\varphi & \cos\varphi \end{bmatrix} \tag{3}$$

Having thus described a new coordinate system for the hand, we now find a combination of joint inputs to move the hand along the vectors $\hat{\mathbf{u}}_1$ and $\hat{\mathbf{u}}_2$. Rotating the coordinate system for joint space, we can define a new coordinate system given by the unit vectors $\hat{\mathbf{v}}_1$, $\hat{\mathbf{v}}_2$, and $\hat{\mathbf{v}}_3$, so an input along $\hat{\mathbf{v}}_1$ results in motion of the hand along $\hat{\mathbf{u}}_1$, and an input along $\hat{\mathbf{v}}_2$ results in motion along $\hat{\mathbf{u}}_2$. This rotation can be mathematically represented in matrix form as

$$\mathbf{V} = [\,\hat{\mathbf{v}}_1\ \hat{\mathbf{v}}_2\ \hat{\mathbf{v}}_3] \tag{4}$$

A joint velocity along $\hat{\mathbf{v}}_3$ results in a change in the arm's configuration, without producing any hand motion. This is known as a homogeneous solution, and is a characteristic of articulated figures that possess more joints than the desired output requires.[18]

If the original problem described in Equation 1 is formulated for these new coordinate systems, we get

$$\mathbf{U}^T\dot{\mathbf{x}} = \mathbf{D}\,\mathbf{V}^T\dot{\theta} \tag{5}$$

where $\mathbf{U}^T\dot{\mathbf{x}}$ represents the desired hand velocity in the $\hat{\mathbf{u}}_1$, $\hat{\mathbf{u}}_2$ coordinate system; $\mathbf{V}^T\dot{\theta}$ represents the joint velocity in the $\hat{\mathbf{v}}_1$, $\hat{\mathbf{v}}_2$, $\hat{\mathbf{v}}_3$ coordinate system; and **D** is a diagonal matrix of the form

$$\mathbf{D} = \begin{bmatrix} \sigma_1 & 0 & 0 \\ 0 & \sigma_2 & 0 \end{bmatrix} \tag{6}$$

The values σ_1 and σ_2 are known as the singular values and are identically equal to one half the length of the major and minor axes, respectively, of the ellipse in Figure 3. These three matrices **U**, **V**, and **D** provide the singular value decomposition of the Jacobian transformation, so that

$$\mathbf{J} = \mathbf{U}\mathbf{D}\mathbf{V}^T \tag{7}$$

It is also common to write the singular value decomposition as the summation of vector outer products, which for an arbitrary Jacobian would result in

$$\mathbf{J} = \sum_{i=1}^{\min(m,n)} \sigma_i \hat{\mathbf{u}}_i \hat{\mathbf{v}}_i^T \tag{8}$$

where m and n are the number of rows and columns of **J**, and the singular values are typically ordered from largest to smallest.

The singular values, specifying how a transformation scales different vectors between the input space and the output space, are crucial in determining how round-off error has been magnified. In particular, the condition number of a transformation, denoted by κ, is defined as

$$\kappa = \frac{\sigma_{max}}{\sigma_{min}} \tag{9}$$

The condition number is important because it provides a bound on the worst case magnification of relative errors. To see why this is true, consider the case where the solution of Equation 1 is desired for a given $\dot{\mathbf{x}}$. If the uncertainty in $\dot{\mathbf{x}}$ is denoted by $\delta\dot{\mathbf{x}}$, then the range of possible values of $\dot{\mathbf{x}} + \delta\dot{\mathbf{x}}$ defines a circle in hand space, as illustrated in Figure 4. Transforming this circle into joint space results in an ellipse in joint space with minor and major axes aligned with $\hat{\mathbf{v}}_1$ and $\hat{\mathbf{v}}_2$ and of magnitude equal to the reciprocals of their respective singular values. The relative uncertainty in the solution is therefore bounded by

$$\frac{\|\delta\dot{\theta}\|}{\|\dot{\theta}\|} \leq \kappa \frac{\|\delta\dot{\mathbf{x}}\|}{\|\dot{\mathbf{x}}\|} \tag{10}$$

It is easy to verify that the worst case denoted by the equality will occur if $\dot{\mathbf{x}}$ is entirely along $\hat{\mathbf{u}}_1$, and $\delta\dot{\mathbf{x}}$ is entirely along $\hat{\mathbf{u}}_2$. A similar bound can be determined for the relative error magnification in the calculation of the Jacobian itself. Thus, by monitoring the maximum and minimum singular values, we can assess how confident we can be in a computed result.

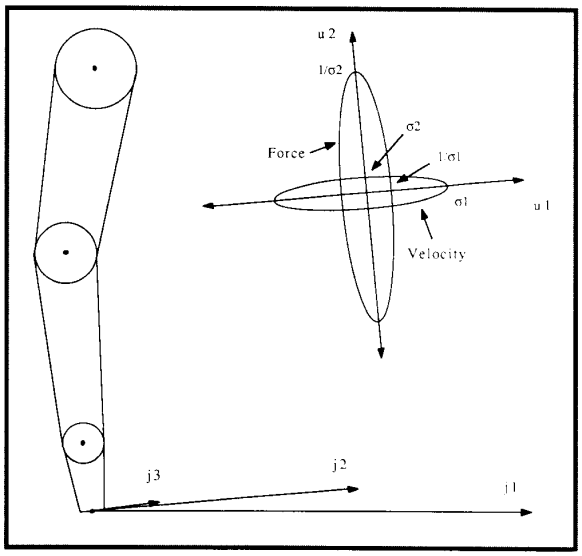

Figure 5. The physical effects of approaching a singularity. The achievable velocity of the hand becomes restricted to the nonsingular direction. However, because of the duality of the static force and velocity relationships defined by the Jacobian, the singularity also results in the ability to balance large forces in the singular direction.

Singularities and pseudoinverse solutions

The above discussion shows that the minimum singular value is important in determining the conditioning of the Jacobian and therefore in obtaining usable solutions to Equation 1. Since the conditioning of Equation 1 becomes worse as σ_{min} decreases, we should consider the worst case—what happens when σ_{min} is equal to zero. Then $\mathbf{J}$ is referred to as singular, and an exact solution to Equation 1 will not exist for an arbitrary desired hand velocity.

To examine the physical significance of this situation, consider the configuration of the arm shown in Figure 5. The arm is approaching the singular configuration of being completely stretched out. Joint rotations about each of the three joints result in approximately the same motion at the hand; in mathematical terms the joints are becoming linearly dependent. Note that it becomes increasingly easier to move in the direction of $\hat{\mathbf{u}}_1$, while velocities along $\hat{\mathbf{u}}_2$ become increasingly more difficult. At the actual singularity there is no combination of joint velocities that can result in a hand velocity along $\hat{\mathbf{u}}_2$.

Pseudoinverses are commonly used to obtain meaningful solutions to singular (or nonsquare) systems of equations. The pseudoinverse solution is the best possible approximation, since it results in the least-squares solution. This is defined as minimizing the residual given by $\|\dot{\mathbf{x}} - \mathbf{J}\dot{\theta}\|$, which physically means that the hand velocity will be as close to the desired velocity as possible. Minimization of the residual does not of itself guarantee a unique solution.

The pseudoinverse solution is unique in that it also minimizes the norm of the solution; that is, it minimizes the amount of joint motion under the constraint of minimizing the residual. In effect, this means that there is no unnecessary motion in achieving the desired hand trajectory.

It is also possible to use formulations based on the pseudoinverse that sacrifice the minimum-norm criterion to achieve other desirable characteristics.[17] The pseudoinverse solution is very easily obtained from the singular value decomposition by taking the reciprocal of all nonzero singular values. In particular, the pseudoinverse of $\mathbf{J}$, denoted by $\mathbf{J}^+$, is given by

$$\mathbf{J}^+ = \sum_{i=1}^{r} \frac{1}{\sigma_i} \hat{\mathbf{v}}_i \hat{\mathbf{u}}_i^T \tag{11}$$

where r is the rank of $\mathbf{J}$ that is by definition the number of nonzero singular values.

The ability of the pseudoinverse to provide meaningful solutions to any linear system of equations—regardless of whether it is underspecified,

overspecified, or even singular—accounts for its popularity in the literature.[2-4,7,11-14,17,18] However, using true pseudoinverse solutions for any equations describing the motion of articulated figures still has fundamental drawbacks. Such equations are not isolated mathematical formulas, but represent how the physical system evolves over time. As such, we are repeatedly solving sets of equations slightly perturbed from the previous set of equations. Physically, their solutions must have continuity, and here the pseudoinverse solutions fail.

As an example, consider the singular value decomposition of the Jacobian for the arm in Figure 5, where the diagonal matrix of singular values is given by Equation 6. While σ_2 remains nonzero, the pseudoinverse of **D** will be given by

$$\mathbf{D}^+ = \begin{bmatrix} \frac{1}{\sigma_1} & 0 \\ 0 & \frac{1}{\sigma_2} \\ 0 & 0 \end{bmatrix} \tag{12}$$

However, when the arm moves into the singular configuration and σ_2 becomes zero, the pseudoinverse becomes

$$\mathbf{D}^+ = \begin{bmatrix} \frac{1}{\sigma_1} & 0 \\ 0 & 0 \\ 0 & 0 \end{bmatrix} \tag{13}$$

The difficulty therefore is not *at* the singularity, where the pseudoinverse provides a perfectly reasonable solution, it is the *discontinuous transition* between singular and nonsingular configurations. Unfortunately, at this transition the equations are also most ill conditioned. Furthermore, even if the equations could be solved exactly, using Equation 12 for $\sigma_2 \rightarrow 0$ results in solution norms that approach infinity. Such spikes and oscillations in the derivatives of the joint positions tend to wreak havoc with numerical integration routines.

The large norm of pseudoinverse solutions characteristic of proximity to singularities may at first seem paradoxical for a technique guaranteed to yield the minimum-norm solution. This apparent paradox is resolved by noting that the least-squares criterion of achieving the hand trajectory takes priority over minimizing the joint velocity. Thus the solution of minimum norm is chosen only from those solutions already satisfying the least-squares criterion. This explains the discontinuity in pseudoinverse solutions at singularities, since it represents a switch in the optimization criterion. The decrease in rank encountered at a singularity means that a component of joint angle motion can no longer be used to improve the least-squares criterion. Instead it is applied to the minimum-norm criterion. Thus one method of removing this discontinuity and also limiting the maximum solution norm is to consider both criteria simultaneously.

A well-conditioned formulation

Considering a solution's norm along with the accuracy to which it solves a set of linear equations was first proposed by Kenneth Levenberg in 1944, in a technique he called "damped least squares." He pointed out that the iterative solutions of linear equations resulting from nonlinear systems, such as the equations of motion for articulated figures, are valid only near the current operating point. Physically, then, it makes sense to consider only solutions that lie in this vicinity. Damped least squares, also called regularization, has become one of a number of common techniques for solving ill-conditioned equations in various disciplines.

In terms of solving Equation 1, the damped least-squares criterion is based on finding the solution that minimizes the sum

$$\| \dot{\mathbf{x}} - \mathbf{J}\dot{\theta} \|^2 + \lambda^2 \| \dot{\theta} \|^2$$

where λ, sometimes referred to as the damping factor, weights the importance of minimizing the joint velocity with respect to minimizing the residual. This criterion results in the augmented system of equations

$$\begin{bmatrix} \mathbf{J} \\ \lambda \mathbf{I} \end{bmatrix} \dot{\theta} = \begin{bmatrix} \dot{\mathbf{x}} \\ 0 \end{bmatrix} \tag{14}$$

where the solution can be obtained by solving the consistent set of equations

$$(\mathbf{J}^T\mathbf{J} + \lambda^2\mathbf{I})\, \dot{\theta} = \mathbf{J}^T\dot{\mathbf{x}} \tag{15}$$

which results in the damped least-squares solution, denoted here by $\dot{\theta}^{(\lambda)}$. The physical significance of this $\dot{\theta}^{(\lambda)}$ is that it is the unique solution most closely achieving the desired hand trajectory from all possible combinations of joint velocities that do not exceed $\| \dot{\theta}^{(\lambda)} \|$.

We again use singular value analysis to see how the damped least-squares formulation resolves the discontinuity present with pseudoinverse solutions. The singular value decomposition of the damped least-squares transformation obtained from Equation 15 is given by

$$(\mathbf{J}^T\mathbf{J} + \lambda^2\mathbf{I})^{-1}\mathbf{J}^T = \sum_{i=1}^{r} \frac{\sigma_i}{\sigma_i^2 + \lambda^2}\hat{\mathbf{v}}_i\hat{\mathbf{u}}_i^T \tag{16}$$

Comparing the singular value decomposition of this solution to the one given by the pseudoinverse in Equation 11 shows they are very closely related. In fact, the damped least-squares formulation can be seen as a generalization of the pseudoinverse, since the pseudoinverse can be obtained by simply setting $\lambda = 0$.

For cases where the damping factor is not equal to zero, consider the form of the damped least-squares solution as a function of the singular values. If a singular value is much larger than the damping factor, then the damped least-squares formulation has little effect, because

$$\frac{\sigma_i}{\sigma_i^2 + \lambda^2} \approx \frac{1}{\sigma_i} \tag{17}$$

which is identical to the solution obtained using the pseudoinverse. For singular values on the order of λ, the λ term in the denominator "damps" the potentially high norm of that component of the solution, so the maximum scaling for this component is limited by

$$\frac{\dot{\theta}_i^{(\lambda)}}{\dot{x}_i} \leq \frac{1}{2\lambda} \tag{18}$$

where the subscript i denotes the components associated with the ith singular value. The maximum joint velocity represented by the equality in Equation 18 will occur when $\sigma_i = \lambda$. If the singular value continues to decrease and becomes much smaller than the damping factor, then

$$\frac{\sigma_i}{\sigma_i^2 + \lambda^2} \approx \frac{\sigma_i}{\lambda^2} \tag{19}$$

which approaches zero as the singular value approaches zero. This demonstrates the required continuity in the solution, despite the change in rank at the singularity. Figure 6 plots the form of the damped least-squares solution, illustrating this continuity as compared with the pseudoinverse solution.

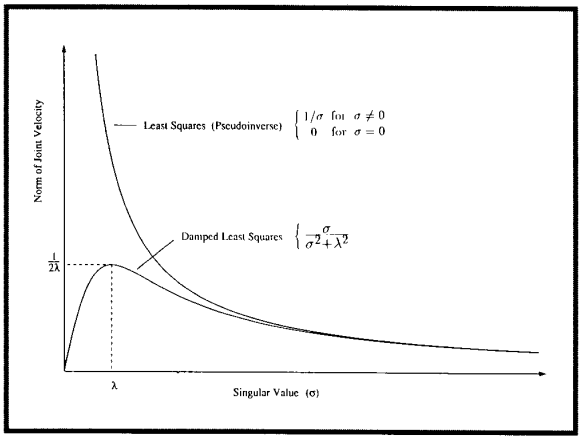

Figure 6. A comparison of the damped least-squares solution to that of the pseudoinverse as a function of the singular value. The maximum possible value of the joint velocity is determined by the damping factor λ. The damped least-square solution also resolves the discontinuity of the pseudoinverse solution at a singularity ($\sigma = 0$).

In addition to resolving the problem of discontinuities, the damped least-squares formulation can be made arbitrarily well conditioned by choosing an appropriate damping factor. Consider the conditioning of the implicit inversion of the matrix $\mathbf{J}^T\mathbf{J} + \lambda^2\mathbf{I}$ in Equation 15. It is easy to show that the condition number of this $n \times n$ matrix, denoted by κ_{dls}, is given by

$$\kappa_{dls} = \frac{\sigma_1^2 + \lambda^2}{\sigma_n^2 + \lambda^2} \tag{20}$$

Thus, regardless of the conditioning of the original problem, recasting the formulation to include physically realistic constraints on the solution guarantees reasonable results.

To obtain an efficient algorithm and to avoid introducing numerical instability, many issues must be considered when actually calculating the damped least-squares solution. These issues, beyond the scope of this introductory presentation, have been discussed in detail in the literature. An appropriate damping factor can be automatically selected and the damped least-squares solution calculated without resorting to the singular value decomposition.[19] Also, the iterative nature of the motion equations for articulated figures can reduce the computational complexity of calculating the singular value decomposition.[20]

Dynamics simulations

This section gives an example of how to use the damped least-squares formulation to simulate the dynamics of articulated figures. Regardless of the formulation used, the equations describing the dynamics of an articulated figure can be cast in the form

$$\tau = \mathbf{H}(\theta)\ddot{\theta} + \mathbf{c}(\theta,\dot{\theta}) + \mathbf{g}(\theta) + \mathbf{J}(\theta)^T f \quad (21)$$

where τ is an n-dimensional vector of the torques at the joints, and $\mathbf{H}(\theta)$ is an $n \times n$-dimensional symmetric matrix of inertias, which is a configuration-dependent combination of the individual link masses and inertia tensors. Here $\mathbf{c}(\theta, \dot{\theta})$ is an n-dimensional vector of centrifugal and Coriolis torques, $\mathbf{g}(\theta)$ is an n-dimensional vector that represents the joint torques due to gravity, and $\mathbf{f}$ is an m-dimensional vector of the external generalized forces acting on the figure, which is transformed into joint torques by the transpose of the $m \times n$-dimensional Jacobian. The torques due to $\mathbf{c}$, $\mathbf{g}$, and $\mathbf{f}$ are known, so the simulation equation becomes

$$\tilde{\tau} = \mathbf{H}(\theta)\ddot{\theta} \quad (22)$$

where

$$\tilde{\tau} = \tau - \mathbf{c}(\theta, \dot{\theta}) - \mathbf{g}(\theta) - \mathbf{J}(\theta)^T\mathbf{f} \quad (23)$$

The typical simulation problem is to solve Equation 22 for a given set of torques at the joints to obtain the joint accelerations. They are then integrated to obtain the joint velocities and positions. The numerical integration of these calculated joint accelerations can create difficulties. While the matrix of inertias $\mathbf{H}$ cannot be singular for the physical reasons cited above, it can become very ill conditioned. The larger the dimension of $\mathbf{H}$ and the greater the disparity between the masses and inertia tensors of the individual links, the more likely it becomes that $\mathbf{H}$ will be ill conditioned. When this occurs, the calculated acceleration may vary, because the uncertainties involved are magnified. At its worst, this situation will prevent the integration routine from working at all; at best the routine will require a very small integration interval, leading to the excessive computational cost cited in the literature.

To see how the damped least-square formulation can alleviate these difficulties, first note the similarity between Equations 22 and 1. They both require the inverse of some linear transformation to obtain a derivative of joint position. This is then integrated to obtain the configuration of the articulated figure. In many ways, dealing with Equation 22 is numerically preferable because $\mathbf{H}$ is square, symmetric, and nonsingular, as compared with $\mathbf{J}$, which is of arbitrary dimension and rank. However, the discussion of conditioning and the derivations above apply equally well when $\dot{\mathbf{x}}$, $\mathbf{J}$, and $\dot{\theta}$ are replaced by τ, $\mathbf{H}$, and $\ddot{\theta}$. Thus the damped least-squares solution can be applied to guarantee that the norm of the accelerations at the joints will remain within any desired bound. This bound can be determined by either empirical data that specifies the maximum physically achievable acceleration for the figure or by the desired value of the integration interval.

For an illustration, assume that the maximum acceleration for one component of the solution is given, based on the some physical constraint. This value, along with the known value of the torque for this component, is used in Equation 18 to select an appropriate damping factor. Solving Equation 22 with this value of the damping factor guarantees that the resulting joint acceleration component will not exceed the given physical value. In addition, since this bound is guaranteed, the integration interval can be chosen accordingly.

Comparing the damped least-squares solutions with alternative techniques described in the literature is instructive. Armstrong, Green, and Lake suggest scaling all moments of inertia on the basis of physical arguments relating the integration interval to the oscillation frequency of a pendulum.[6,15] The damped least-squares approach is similar in that both techniques artificially increase the effective moments of inertia; however, the difference lies in how these inertias are increased. The damped least-squares solution *adds* to the moment-of-inertia terms that lie along the diagonal of $\mathbf{H}^T\mathbf{H}$, instead of scaling (multiplying) all moments of inertia. Both techniques allow an increase in the integration interval, because they decrease the maximum frequency component of the system. The ratio of the components in the system, however, is altered only by the damped least-squares approach, which accounts for its ability to improve system conditioning. The addition of mass to selected system components allows us to filter out the high-frequency components, which require the small integration intervals, while not appreciably altering the other components in the bulk of the dynamics. Thus the damped least-squares formulation results in the optimal solution, because it most closely matches the system dynamics for a given bound on the allowable acceleration.

Conclusions

Realistic motion simulation for articulated figures requires careful consideration of various numerical issues for a robust and efficient implementation. Both the kinematic and dynamic equations of motion for articulated figures can become very ill conditioned, with the additional complication of becoming singular in the kinematic case. This ill conditioning is inherent in the physical structure of the figure being simulated and cannot be avoided with alternate formulations.

The severity of the situation can be assessed with singular value analysis. While pseudoinverse solutions have been proposed to alleviate some of these numerical difficulties, they have serious drawbacks. In particular, both kinematic and dynamic simulations require numerical integration of quantities obtained from the repeated solution of a perturbed linear system of equations. For this integration to proceed correctly and efficiently, we must avoid spurious values in the quantities being integrated. The damped least-squares formulation avoids such values. By incorporating meaningful bounds on the quantities being integrated, this technique allows a faithful representation of figure kinematics or dynamics, while preventing difficulties in the numerical integration. ■

References

1. D. Zeltzer, "Motor Control Techniques for Figure Animation," *CG&A*, Vol. 2, No. 9, Nov. 1982, pp. 53-60.
2. J.U. Korein and N.I. Badler, "Techniques for Generating the Goal-Directed Motion of Articulated Structures," *CG&A*, Vol. 2, No. 9, Nov. 1982, pp. 71-81.
3. N.I. Badler, K.H. Manoocherhri, and G. Walters, "Articulated Figure Positioning by Multiple Constraints," *CG&A*, Vol. 7, No. 6, June 1987, pp. 28-38.
4. M. Girard, "Interactive Design of 3D Computer-Animated Legged Animal Motion," *CG&A*, Vol. 7, No. 6, June 1987, pp. 39-51.
5. J. Wilhelms, "Using Dynamic Analysis for Realistic Animation of Articulated Bodies," *CG&A*, Vol. 7, No. 6, June 1987, pp. 12-27.
6. W.W. Armstrong, M. Green, and R. Lake, "Near-Real-Time Control of Human Figure Models," *CG&A*, Vol. 7, No. 6, June 1987, pp. 52-61.
7. M. Girard and A.A. Maciejewski, "Computational Modeling for the Computer Animation of Legged Figures," *Computer Graphics* (Proc. SIGGRAPH), Vol. 19, No. 3, July 1985, pp. 263-270.
8. P.M. Isaacs and M.F. Cohen, "Controlling Dynamic Simulation with Kinematic Constraints, Behavior Functions and Inverse Dynamics," *Computer Graphics* (Proc. SIGGRAPH), Vol. 21, No. 4, July 1987, pp. 215-224.
9. M. Moore and J. Wilhelms, "Collision Detection and Response for Computer Animation," *Computer Graphics* (Proc. SIGGRAPH), Vol. 22, No. 4, Aug. 1988, pp. 289-298.
10. J.K. Hahn, "Realistic Animation of Rigid Bodies," *Computer Graphics* (Proc. SIGGRAPH), Vol. 22, No. 4, Aug. 1988, pp. 299-308.
11. A. Witkin and M. Kass, "Spacetime Constraints," *Computer Graphics* (Proc. SIGGRAPH), Vol. 22, No. 4, Aug. 1988, pp. 159-168.
12. R. Barzel and A.H. Barr, "A Modeling System Based On Dynamic Constraints," *Computer Graphics* (Proc. SIGGRAPH 88), Vol. 22, No. 4, Aug. 1988, pp. 179-188.
13. A.H. Barr, R. Barzel, and J.C. Platt, in *Developments in Physically Based Modeling*, SIGGRAPH Course Notes #27, ACM, New York, 1988.
14. D. Zeltzer, in *Synthetic Actors: The Impact of Artificial Intelligence and Robotics on Animation*, SIGGRAPH Course Notes #4, ACM, New York, 1988.
15. W.W. Armstrong and M. Green, "The Dynamics of Articulated Rigid Bodies for Purposes of Animation," *Visual Computer*, Vol. 1, No. 4, Dec. 1985, pp. 231-240.
16. J. Wilhelms, "Toward Automatic Motion Control," *CG&A*, Vol. 7, No. 4, April 1987, pp. 11-22.
17. A.A. Maciejewski and C.A. Klein, "SAM: Animation Software for Simulating Articulated Motion," *Computers and Graphics*, Vol. 9, No. 4, 1985, pp. 383-391.
18. C.A. Klein and C.H. Huang, "Review of Pseudoinverse Control for Use with Kinematically Redundant Manipulators," *IEEE Trans. Systems, Man, and Cybernetics*, Vol. 13, No. 2, March/April 1983, pp. 245-250.
19. A.A. Maciejewski and C.A. Klein, "Numerical Filtering for the Operation of Robotic Manipulators Through Kinematically Singular Configurations," *J. Robotic Systems*, Vol. 5, No. 6, Dec. 1988, pp. 527-552.
20. A.A. Maciejewski and C.A. Klein, "The Singular Value Decomposition: Computation and Applications to Robotics," *Int'l J. Robotics Research*,, Vol. 8, No. 6, Dec. 1989, pp. 63-79.

Anthony A. Maciejewski is an assistant professor of electrical engineering at Purdue University. His research interests include the simulation and control of articulated motion.

Maciejewski received his BSEE, MS, and PhD in electrical engineering from Ohio State University in 1982, 1984, and 1987. He is a member of IEEE and ACM.

Maciejewski can be reached at the School of Electrical Engineering, Purdue University, West Lafayette, IN 47907.